Interpreting Low-Frequency Modes of Southern Hemisphere Atmospheric Variability as the Rotational Response to Divergent Forcing

MICHAEL J. REVELL AND JOHN W. KIDSON

National Institute of Water and Atmospheric Research, Wellington, New Zealand

GEORGE N. KILADIS

NOAA Aeronomy Laboratory, Boulder, Colorado

(Manuscript received 21 September 2000, in final form 6 March 2001)

ABSTRACT

The principal modes of Southern Hemisphere low-frequency variability have recently been calculated using a 39-yr record of 300-hPa streamfunction fields from the NCEP–NCAR reanalysis dataset. The authors attempt to interpret these modes as the rotational response to some divergent forcing. For a range of mean states the linearized barotropic vorticity equation (BVE) is used to solve for the divergent wind that would generate (or at least be consistent with) the observed vorticity modes. Several of these low-frequency modes can be generated by forcing the BVE with fairly simple divergent wind fields that could easily be interpreted as resulting from anomalous tropical convection. In particular this is found to be true for streamfunction anomalies with El Niño–Southern Oscillation (ENSO), high-latitude mode, South Pacific wave, and Madden–Julian oscillation structure. The authors speculate that it may be possible to relate these calculated divergent wind fields to recently observed OLR fields and hence explain some of the variance of the next month's 300-hPa streamfunction by solving the inverse problem.

These results are further evidence that linear Rossby wave propagation provides an important link between anomalous convection in the Tropics and the occurrence of circulation anomalies in higher latitudes.

1. Introduction

Is it possible to predict seasonal flow anomalies in the mid- to high latitudes given prior knowledge of existing patterns of tropical convection? Over the last 20 years there have been many studies establishing the existence of global teleconnection patterns arising from tropical sea temperature anomalies associated with El Niño–Southern Oscillation (ENSO) events. A recent review of this work is contained in Trenberth et al. (1998). The generally accepted explanation has warm (cold) sea temperature anomalies leading to enhanced (diminished) tropical convection and upper-level divergence (convergence). This upper-level divergent flow can excite Rossby waves directly or by interacting with the subtropical jets and these propagate into higher latitudes guided by the background flow. The studies by Horel and Wallace (1981), Hoskins and Karoly (1981), Hoskins and Ambrizzi (1993), Rasmusson and Mo (1993), Tyrrell et al. (1996), and Ambrizzi and Hoskins (1997) provide support for pieces of this overall picture.

Recently Renwick and Revell (1999) presented observational and modeling evidence that blocking in the South Pacific could be the result of a preferred Rossby wave path, originating in the subtropical jet just west of Australia and extending south and east to South America, forced by a dipole of divergence and convergence in the Tropics. The strong suggestion is that this blocking pattern is the rotational response to a particular divergent forcing in the Tropics.

Kidson (1999, hereafter referred to as K99) has calculated the principal modes of Southern Hemisphere (SH) low-frequency variability using a 39-yr record of 300-hPa streamfunction fields from the National Center for Environmental Prediction–National Center for Atmospheric Research (NCEP–NCAR) reanalysis dataset. In this paper we attempt to interpret some of these modes as the rotational response to some divergent forcing. For a range of mean states we use the linearized barotropic vorticity equation (BVE) to solve for the divergent wind that would generate the observed vorticity modes. This problem, hereafter referred to as the χ problem, consists of solving an elliptical equation for the velocity potential χ that would make the given streamfunction ψ a solution of the BVE as explained in Sardeshmukh and Hoskins (1987, hereafter referred to as

Corresponding author address: Dr. M. J. Revell, National Institute of Water and Atmospheric Research Wellington, P.O. Box 14901, Wellington, New Zealand.
E-mail: m.revell@niwa.cri.nz

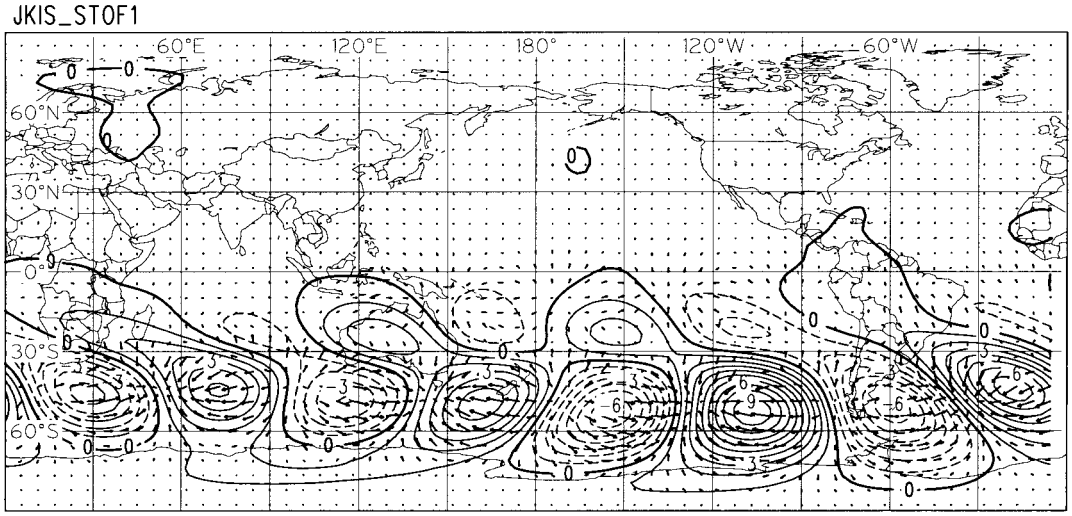

FIG. 1. Streamfunction for the 300-hPa IS1 mode and divergent wind vectors corresponding to the solution of the χ problem for a Sep–Feb mean 300-hPa flow. Contours are every 1.0 $m^2\ s^{-2}$ with wind vectors of one grid length equal to 1 m s^{-1}.

SH87). If we could robustly associate these midlatitude streamfunction anomalies with an unambiguous tropical divergent signal it would be a useful first step in answering our opening question.

In the next section we describe the datasets. We describe the BVE model in section 3 and present a solution method for the linearized χ problem. In section 4 we first present the observed principal modes of low-frequency variability in the circulation of the SH. We do this for both 11-month running mean and 10–120-day bandpass-filtered datasets in an attempt to separate ENSO and Madden–Julian oscillation (MJO) signals. We then present the model χ solutions for each of the modes and a range of background states. A general discussion of results is given in the final section.

2. Data

Calculation of the principal modes of low-frequency variability in the SH extratropics is based on a 39-yr (Jan 1958–Jun 1997) time series of twice-daily 300-hPa winds from the NCEP–NCAR reanalysis project (Kalnay et al. 1996). A full discussion of the strengths and weaknesses of the dataset and method of determining the principal empirical orthogonal functions (EOFs) is given in K99. Here we just summarize the key elements of the method. The most significant patterns of streamfunction variation are presented in section 4.

In contrast to many previous studies the analysis was performed on the streamfunction, giving equal weight to velocities in the Tropics and extratropics. The analysis area was limited to the SH rather than the global domain, in contrast to the earlier analysis of Lau et al. (1994), in order to concentrate on SH variability. Global patterns for use in the BVE were obtained as the covariance of the time series of each EOF with the global streamfunction fields. The resulting patterns, with the exception of those originating in the Tropics, confirm the lack of any consistent coupling between variations in midlatitudes in the SH and those in the Northern Hemisphere (NH).

The wind data were sampled twice daily, and fast Fourier transformed into a streamfunction field. A subset of points was extracted at 5° resolution in latitude and at variable resolution in longitude (fewer point toward the pole) to avoid biasing the results toward the polar regions. In order to separate intraseasonal (IS) and interannual (IA) variability, 10–50-day bandpass and 50-day lowpass filters were then applied to the streamfunction fields. A further partitioning into intradecadal (ID) and interannual-monthly (IAM) components was achieved by taking 11-month running means of the lowpass-filtered data and subtracting these from the individual monthly means, respectively.

Finally, in order to highlight MJO signals a combined EOF analysis of outgoing longwave radiation (OLR) between 30°N and 30°S and 200-hPa streamfunction between 0° and 90°S was performed. This was not done in K99. After bandpass filtering between 10 and 20 days, the OLR was normalized by dividing by the area average standard deviation of OLR between 30°N and 30°S and similarly for the streamfunction between 0° and 90°S. These were combined by weighting by the square root of the cosine of latitude, giving equal weight to both fields and an EOF analysis of the covariance matrix was performed on a 10° grid. The results were found to be insensitive to resolution with 2.5° data giving the same answer. Again global data for use in the BVE model were produced as above.

The above EOF analysis produced modes in various frequency ranges. They are displayed in full in K99 and

examples of those analyzed in this paper will be presented in section 4.

3. Model and solution of the χ problem

Can the midlatitude circulation anomalies defined by the EOF analysis in the previous section be interpreted as a linear Rossby wave response to some observable tropical convective anomaly? In other words if we interpret the patterns discovered in the previous section as low-frequency streamfunction anomalies superimposed on some mean flow, can we calculate the divergent flow required to make them a solution of the linearized BVE? SH87 have shown that in general it is possible to solve the BVE for ψ given χ (the psi problem) or χ given ψ (the chi problem). Much of the following derivation can be found in or deduced from SH87; however for completeness, we outline here the method for the linearized problem.

The model

The barotropic model, used to calculate the divergent wind required to force the observed low-frequency rotational wind anomalies, solves for the vertical component of the vorticity equation, which, neglecting vertical advection and twisting terms, can be written as

$$\frac{\partial \xi}{\partial t} = -\nabla \cdot [\mathbf{v}\zeta] + \lambda(\xi_0 - \xi) + \mu\nabla^6\xi. \qquad (1)$$

In (1), ξ is the relative vorticity, f is the Coriolis parameter, ζ is the absolute vorticity ($\xi + f$), and $\mathbf{v}$ is the wind vector with $\mathbf{v}_\psi$, $\mathbf{v}_\chi$ being the rotational and divergent components, μ determines the timescale over which the shortest length scale is dissipated, and λ determines the timescale over which ξ is relaxed back to the mean $\overline{\xi}$.

We separate the wind $\mathbf{v}$ into its rotational and divergent components $\mathbf{v}_\psi$, $\mathbf{v}_\chi$ and introduce a velocity potential χ, such that $\mathbf{v}_\chi = \nabla\chi$ and the horizontal divergence $D = \nabla^2\chi$. Putting the divergence terms on the left, we can write (1) above as

$$\nabla \cdot (\mathbf{v}_\chi\zeta) = \zeta\nabla^2\chi + \nabla\zeta \cdot \nabla\chi$$
$$= -\mathbf{v}_\psi \cdot \nabla\zeta - \frac{\partial \xi}{\partial t} + \lambda(\xi_0 - \xi) + \mu\nabla^6\xi. \qquad (2)$$

Linearizing (2) about a climatological mean state, denoted by an overbar with anomalies denoted by primes, we get

$$\overline{\zeta}\nabla^2\chi + \nabla\overline{\zeta} \cdot \nabla\chi = F, \qquad (3)$$

where

$$F = -\mathbf{v}'_\psi \cdot \nabla\overline{\zeta} - \overline{\mathbf{v}}_\psi \cdot \nabla\xi' - \frac{\partial \xi'}{\partial t} - \lambda\xi' + \mu\nabla^6\xi'. \qquad (4)$$

All the terms in (4) are known, since the overbarred terms correspond to the climatological mean state, the primed terms to the rotational modes of variability. The dissipation term is not needed for convergence, but was included to make the process an exact inverse of the psi problem. Using daily vorticity values we initially calculated the tendency term, but found the results to be very insensitive to its inclusion, so we subsequently assumed the tendency term to be small. Now we have an elliptic equation for the velocity potential χ, which can be solved essentially by relaxation as follows.

We rewrite (3) as

$$G = F - \overline{\zeta}\nabla^2\chi - \nabla\overline{\zeta} \cdot \nabla\chi, \qquad (5)$$

make a first guess at the divergence D, and then refine it iteratively until the remainder G is sufficiently small. Successive guesses at D are given by

$$D^{i+1} = D^i + \delta\overline{\zeta}G^i \qquad (6)$$

where i is the iteration index, δ is a constant with dimensions of time, and the factor ζ (which has opposite signs in each hemisphere) has been introduced in order to give convergence in both hemispheres. We are in effect looking for solutions to the equation

$$\partial D/\partial t = \overline{\zeta}G, \qquad (7)$$

which apart from the factor ζ is mathematically similar to the barotropic vorticity equation with forcing. We have in fact, like SH87, used the same computer code to solve it with only minor modifications. A forward time step of 0.5 h was found to be stable for T42 truncation. We solved for all spectral components with total wavenumber $\leq$21. As explained in SH87, convergence can be slow at the equator, where solutions from the two hemispheres are being matched, and it was found up to 400 iterations were sometimes needed.

The method was checked for accuracy and robustness by taking one of the solutions to the ψ problem given in Renwick and Revell (1999) and rederiving the divergence field that forced it. The fields agreed very well—to better than 1 part in 20.

4. EOF and model results

We now introduce the modes discovered by the EOF analysis described in section 2 and present solutions to the χ problem for several of them. Initially all our model calculations use the September to February mean flow as the background state as this has been shown to be when ENSO-related tropical heating anomalies have their peak (Mitchell and Wallace 1996). We also did calculations using background states based on individual months (Oct, Jan, Apr, and July) and found quite marked differences in the Northern Hemisphere between summer and winter because of the disappearance of the Asian jet. In the Southern Hemisphere however the seasonal variation was considerably less. Sensitivity to this will be commented on as appropriate.

The BVE has been applied at the 300-hPa level for

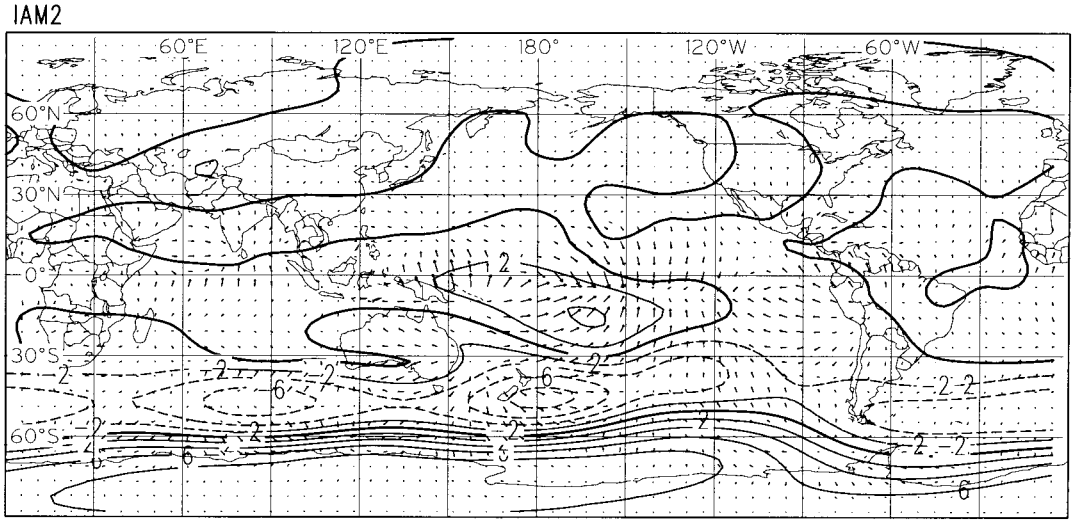

FIG. 2. As in Fig. 1 but for the IAM2 or high-latitude mode.

intraseasonal, interannual-monthly and intradecadal modes and at the 200-hPa level for the 10–120-day modes corresponding to the levels at which the EOF analysis was done. The appropriateness of these levels for single-level studies has been discussed by Jin and Hoskins (1995), who considered the response of a baroclinic atmosphere to tropical heating. It is also our experience that the results are not sensitive to the precise level chosen; however, the 200-hPa response gives greater emphasis to the role of Australasian subtropical jet while the 300-hPa response favors the polar jet. In the discussion that follows we refer to divergence and convergence in the text but show corresponding wind vectors in the accompanying figures, as this is clearer than superimposing two contoured fields.

a. Intraseasonal modes

Eastward propagating wavenumber 4 (IS1 and IS2 of K99) and 5 (IS5 and IS6) patterns with significant amplitude confined between 40° and 60°S, the location of the major storm track in the SH (Trenberth 1991), were revealed by EOF analysis of the 10–50-day bandpass-filtered data. The only other significant pattern consisted of wavenumber 4 contributions to the zonal wind variation in the subtropics (IS3 and IS4).

We show mode IS1 from K99 with the required divergent flow depicted as wind vectors in Fig. 1. There is a clear sign of divergence (convergence) ahead of each trough (ridge). This generates precisely the vorticity tendency needed to hold the upper-level component of a barotropic Rossby wave in check and prevent it being torn apart by the vertical shear in the background zonal wind. Thus in this case the solution to the χ problem provides a consistency check but no indication of the forcing coming from the Tropics. This result is typical of other modes in this frequency range, which are not shown.

b. Interannual-monthly modes

After taking 11-month running means of the 50-day low-pass-filtered data and subtracting these from the individual monthly means, EOF analysis of the resulting data produced four main patterns. The first portrays fluctuations in the strength of the subtropical jet. The second is often referred to as the high-latitude mode (HLM) (e.g., Mo and White 1985; Mo 1986; Mo and Ghil 1987; Kidson 1988; Karoly 1990; Kousky and Bell 1992; Kidson and Sinclair 1995; Kiladis and Mo 1998) IAM2 in K99. It describes a zonally symmetric and barotropic alteration in the strength of the zonal wind near 40° and 60°S. The third consists of a zonally orientated pattern over the tropical pacific extending into higher latitudes with alternating sign, referred to as the ENSO mode by K99. The fourth contains a wave train extending from western Australia across the South Pacific to South America, referred to as the Pacific–South American pattern by Mo and Ghil (1987) and by Mo and Higgins (1998) or the South Pacific wave IAM3 and IAM4 in K99. These third and fourth patterns are strongly suggestive of a tropical origin.

From the range of interannual-monthly streamfunction patterns we first consider the IAM2 mode in K99, also there referred to as the high-latitude mode. The corresponding divergent flow, shown in Fig. 2, in the Tropics consists of divergence over South America, East Africa, and east of Papua New Guinea, with convergence in the central Pacific, Indian Ocean, and west Africa—in other words a monsoonlike circulation. The HLM anomaly consists of increased westerlies between 55° and 65°S and reduced westerlies between 35° and

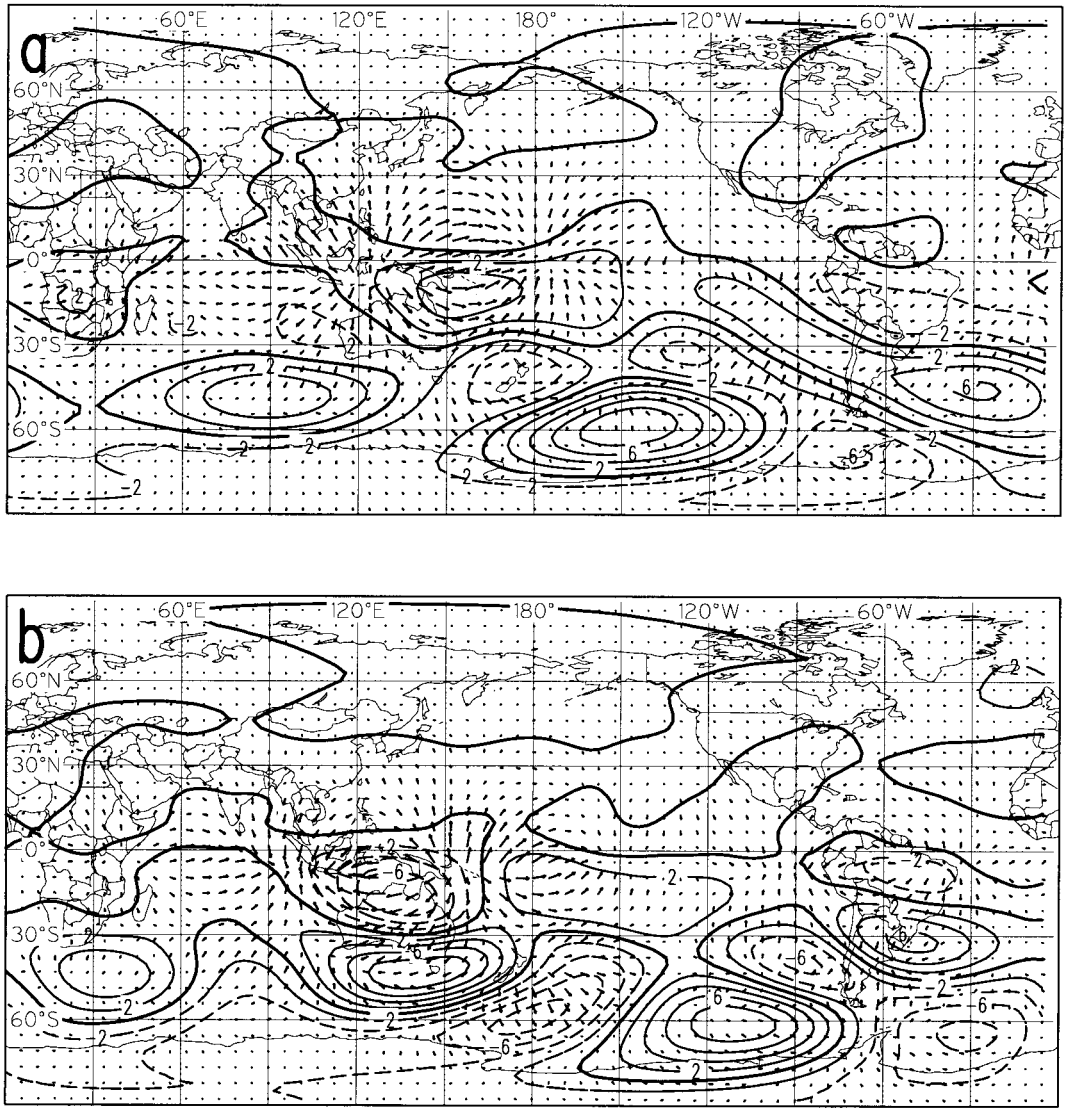

FIG. 3. As in Fig. 1 but for the (a) IAM3 and (b) IAM4 or South Pacific wave mode.

45°S in each of the Pacific, Atlantic, and Indian Ocean basins. The χ anomaly signal corresponds to divergence in the southern regions of each ocean basin and convergence in the tropical pacific—a weakened Hadley and Ferrel circulation in each basin. These circulations imply the above HLM circulation through the Coriolis term in the vorticity equation. The tropical signal is most noticeable in the Pacific sector in the region of the South Pacific convergence zone. Note that this analysis is linear, and what has been described above is just one phase of the HLM. With equal likelihood the signs of the anomalies could all be reversed giving the opposite phase.

The solution to the χ problem does not indicate whether the HLM forces the tropical Hadley anomaly or vice versa; however, it establishes a relationship between them. The observational studies of Kidson and Sinclair (1995) and K99 both indicate that the peak poleward momentum transport associated with the HLM is not increased although it is displaced in latitude. The changes in the zonal mean at higher latitudes do not relate strongly to those in the Tropics; however, Kidson et al. (2000, manuscript submitted to *J. Climate*, hereafter referred to as K00) suggest that the positive phase of the HLM is linked to stronger convection in the South Pacific convergence zone (SPCZ). They find the positive phase of the HLM to be associated with more cloud on the equatorward edge of the SPCZ or perhaps a poleward displacement of its mean position. Recently J. W. Hurrell and M. P. Hoerling (2000, personal communication) have noted a trend in the amplitude of the HLM and heating in the region of the SPCZ. However we have been unable to find a similar trend in four decades of the time series of the IAM2 mode. Further work is

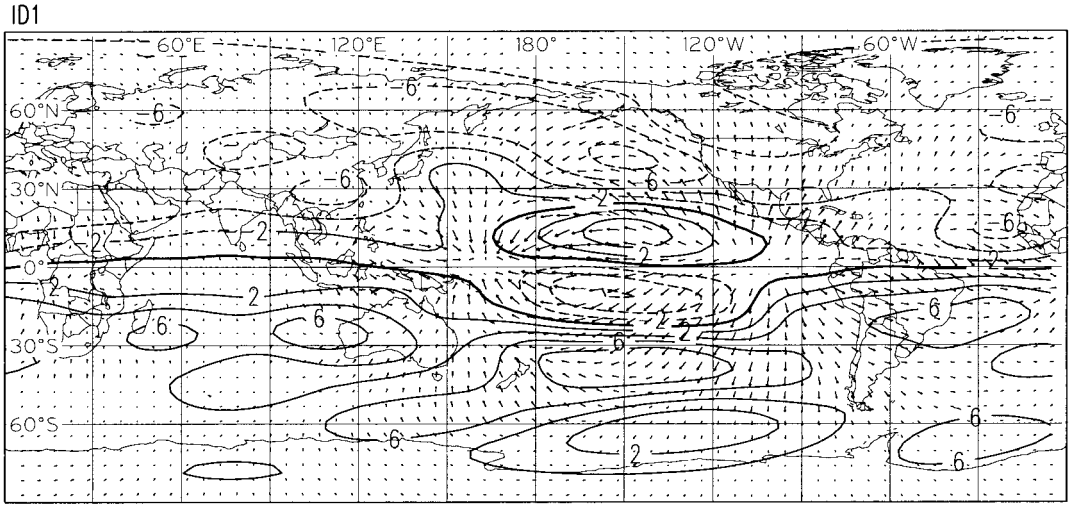

FIG. 4. As in Fig. 1 but for the ID1 or El Niño–Southern Oscillation mode.

needed to determine whether the HLM is modulating convection in the SPCZ or vice versa, but there does appear to be a connection.

Next the IAM3 and IAM4 modes in K99, referred to as the South Pacific Wave (SPW), are shown in Fig. 3 along with the divergent wind vectors obtained from solving the χ problem. A clear tropical dipole anomaly is seen between the date line and just west of Indonesia with similar but much weaker signals over the tropical parts of South America and Africa. IAM3 and IAM4 appear to be different phases of the same wave pattern but shifted by 90°. The IAM3 wave pattern is very similar (with opposite sign) to the wave pattern associated with *blocking* in Renwick and Revell (1999). There is a similar Rossby wave source region (not shown) in the background jet region over western Australia, plus weak source regions along the wave path itself—similar to the IS modes. The wave train starts at a variable location but the wave energy gets into a preferred duct across the Pacific. The phase is important for interannual-monthly climate variability, and it might be possible to predict it, knowing the OLR pattern, by solving the inverse psi problem.

c. Intradecadal modes

EOF analysis of the 11-month means of the 50-day low-pass-filtered data produced only one significant new pattern. The ENSO and HLM signal reappeared, plus a pattern representing a change in circulation before and after 1970.

From these intradecadal streamfunction patterns we consider the ID1 mode in K99, there called the ENSO mode. This is shown in Fig. 4 with the divergent flow corresponding to the χ solution again plotted as wind vectors. The ID1 streamfunction anomalies, particularly the pair of equatorial anticyclones, match up well with the composite El Niño and La Niña patterns from K00. However here the implied vertical motion corresponding to the very clear χ signal in the Tropics, with divergent flow (upward motion) at the eastern end of the streamfunction anomaly and convergence (downward motion) at the western end, does not precisely match the OLR pattern in K00. This χ pattern is consistent with the simple heat-induced tropical circulations presented in Gill (1980), but the OLR patterns in K00 indicate greatest cloudiness and presumably upward motion at about 170°W for El Niño conditions, more or less in the middle of the equatorial anticyclones.

Thus although this streamfunction pattern is clearly established, at the BVE level of approximation, as resulting from the simple divergence pattern shown above, this does not match the corresponding observed OLR pattern. It appears that in the equatorial region the linearized BVE approximation is inadequate for this mode. Hendon (1986) points out that it is important to take account of nonlinearities in order to explain the spatial relationship between the divergence/OLR anomalies and the tropical streamfunction anomalies. We have not done that here and suggest this is the reason for the discrepancy. Using July and January background flows again makes very little difference to the required divergence (not shown for these cases) establishing a robust connection between the tropical divergence and this midlatitude streamfunction anomaly pattern.

d. 10–120-day modes

Since we were particularly interested in the potential for the MJO tropical signal to be used for extended-range forecasting in the New Zealand region, but no clear such signal had appeared in the patterns described above, we also considered cross correlations between tropical OLR and variability of the 200-hPa streamfunction in the SH on 10–120-day timescales for the December to February season. The leading two modes

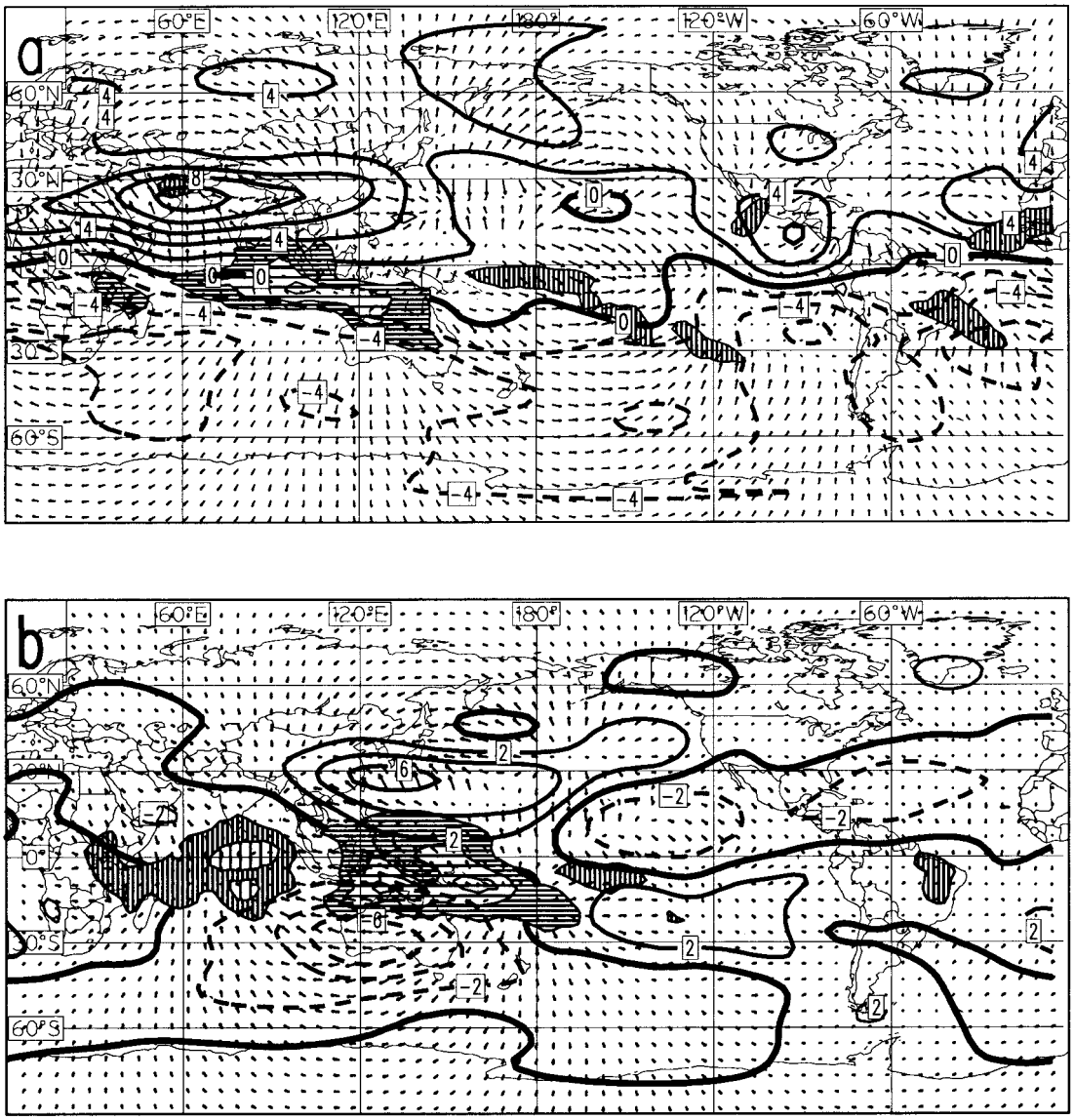

FIG. 5. As in Fig. 1 but for combined EOFs for the two phases (a), (b) of the MJO mode. Hatched regions correspond to the EOFs of OLR with | (−) orientation = positive (negative).

resulting from this calculation appear to be associated with the MJO (Madden and Julian 1972). We show the pair as an active MJO moving from the Indian Ocean in Fig. 5a into the western Pacific in Fig. 5b. The principal components individually have spectral peaks in the 42–48-day range and have a maximum correlation of −0.8, which peaks when Fig. 5a leads Fig. 5b by 12 days, giving a 48-day oscillation.

The MJO is an eastward-propagating disturbance that has its maximum amplitude within the Tropics of the eastern Indian to western Pacific Oceans. It has a broad period range maximizing between 41 and 53 days, and most of the spatial amplitude of the wave is contained within zonal wavenumbers 0 through 2. There is a strong zonally symmetric signal associated with the well known tendency for the MJO to modulate atmospheric angular momentum (Weickmann et al. 1997). Large perturbations in convection and circulation within the Tropics are associated with the disturbance, but significant systematic extratropical circulation signals in both hemispheres are also observed during its evolution.

Solutions of the χ problem for these streamfunction anomalies are also shown in Fig. 5 as wind vectors. The implied divergences match closely the corresponding OLR patterns shown as hatched areas. The streamfunction anomalies have some amplitude in midlatitudes, indicating that it may be possible to make predictions several weeks in advance of particular weather regimes

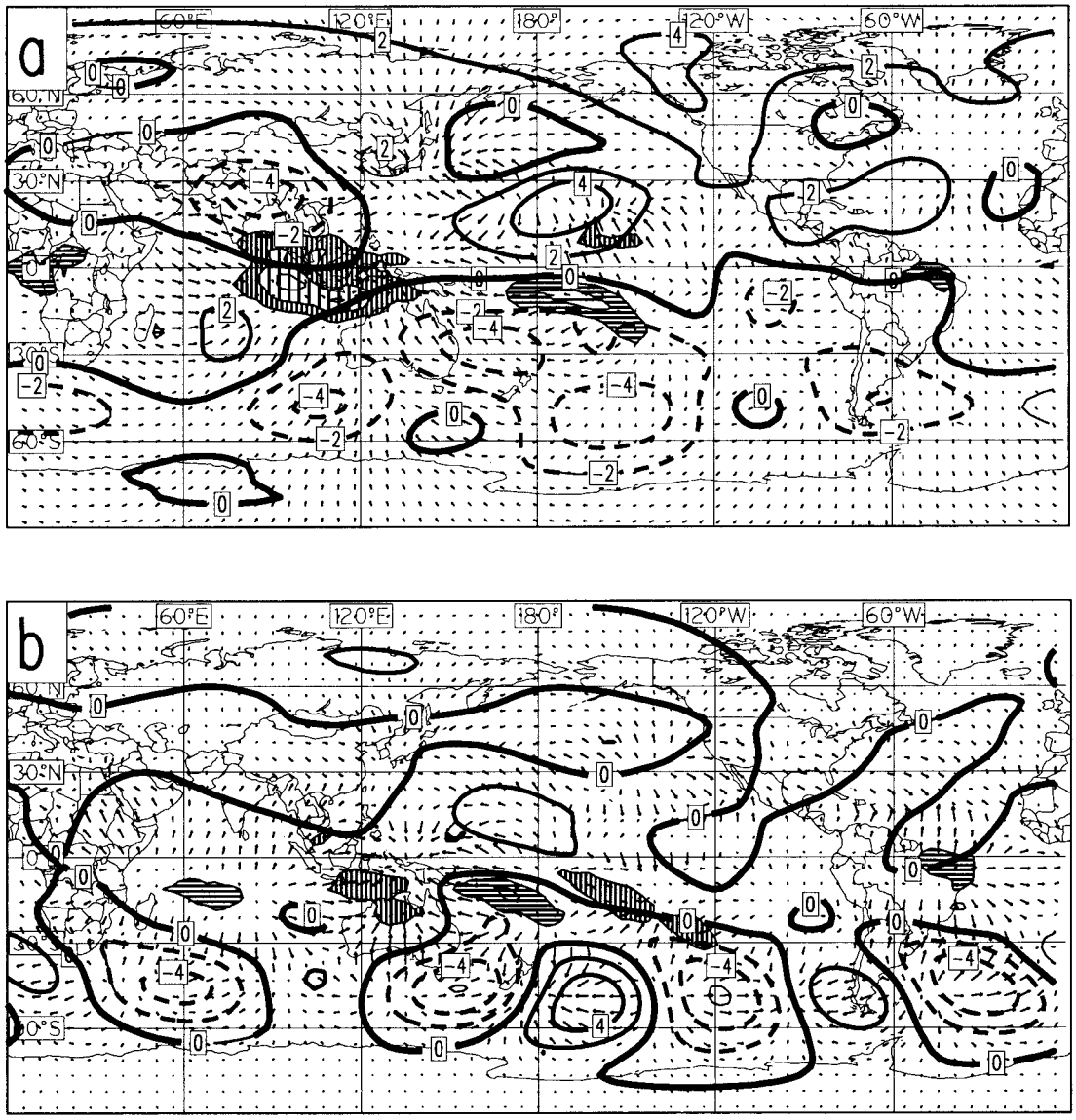

FIG. 6. As in Fig. 5 but for the (a) mixed and intraseasonal (b) and South Pacific wave modes.

if we could measure the current amplitude and phase of the tropical MJO signal, again by solving the inverse psi problem.

The next two EOFs based on the 200-hPa streamfunction calculation are shown in Fig. 6 along with hatching for the corresponding OLR fields and wind vectors indicating solutions of the resulting χ problem. In the SH all the streamfunction patterns are indicative of a Rossby wave train extending from just south and west of Australia across the Pacific under South America and around to South Africa. For mode 3, wind vectors representing solutions to the χ problem indicate enhanced tropical divergence centered near 160°W and convergence centered near 110°E, with weak divergence over Africa and South America—closely matching the hatched areas. For mode 4, the midlatitude wave train and the tropical divergent winds are all displaced about 40°E relative to mode 3. The wavelength of the tropical signal is shorter and there is relatively more divergence in the region of the wave train itself. For mode 3 the Rossby wave source (RWS) regions (not shown) are also in the wave train itself rather than in the vicinity of the jets. This indicates that for mode 4 the RWS is dominated by the divergence of the wind rather than its dot product with the background vorticity [the first and second terms, respectively, on the left-hand side of Eq. (2)]. We suggest these modes are a combination of the SPW mode and the IS1 mode described earlier in K99, since the filtering period of 10–120 days now spans both the intraseasonal and interannual-monthly range. However, including the tropical OLR fields in the analysis has highlighted the MJO modes, which were not obvious

in the analyses of K99, since these were based on data in the SH only.

As a final check on the appropriateness of the BVE approximation to describe tropical midlatitude interactions we computed fields of 200-hPa divergence from monthly velocity potential anomalies and correlated these with the series for the EOFs IS1, IAM2, IAM3, IAM4, and ID1. Outside the 15° tropical belt there was generally very good agreement between the divergences calculated this way and those derived by solving the BVE. In the tropical belt however the divergences derived by correlation were generally small apart from those for the ID1 mode. For this ENSO mode the divergence tended to be largest in the middle of the equatorial anticyclones again suggesting the importance of nonlinear effects in determining the local vorticity balance in the tropical belt as we pointed out in the above discussion of the intradecadal modes.

5. Summary and conclusions

In summary then, we have taken the principal modes of Southern Hemisphere low-frequency variability, recently calculated using a 39-yr record of 300-hPa streamfunction fields from the NCEP–NCAR reanalysis dataset. Moving from higher to lower frequency, but not in equal steps, these modes or teleconnections have become known as intraseasonal modes, the Madden–Julian oscillation, the South Pacific wave, the high-latitude mode, and the El Niño–Southern Oscillation mode. We have attempted to interpret these modes as the rotational response to some pattern of divergent forcing. For a range of mean states, predominantly the austral summer mean flow, since the tropical forcing seems to dominate during this period, we have used the linearized barotropic vorticity equation to solve the χ problem for the divergent wind that would generate, or be consistent with, the above vorticity modes. As shown by SH87 any rotational wind field (one representable by a streamfunction) can be made a steady solution of the BVE by adding a suitable divergent wind field (one representable by a velocity potential). In general, given a streamfunction, solving the χ problem gives a consistent divergent wind field that satisfies the BVE.

We first established the reliability of the method by taking the streamfunction anomaly found by Renwick and Revell (1999) to be associated with South Pacific blocking and rederiving the tropical divergence that forced it. For the IS modes above we found the divergence predominantly in the wave train, with very little suggestion of a tropical source. For this mode, the χ problem is really a consistency check for the divergent wind that makes it a solution of the BVE. For the MJO mode there is a strong clear tropical signal with a wavenumber 1 structure. The streamfunction response is predominantly tropical although there is still some amplitude in the signal at New Zealand latitudes. The SPW mode also produces a clear divergent signal in tropical regions, but this has a shorter wavelength than for the MJO mode. Both the MJO and SPW modes appear to propagate eastward at about 5° per day. The HLM shows convergence (weaker Hadley circulation) over the tropical oceans, particularly the Pacific Ocean in the region of the SPCZ, with matching divergence (weaker Ferrel cell) at about 50°S. However for this mode it is not clear in which direction the interaction takes place. Finally the ENSO mode has the clearest tropical signal of all, with strong divergence (convergence) over the eastern (western) Pacific. For this mode there are differences between the tropical convection implied by the BVE solutions and that implied by observed OLR patterns.

Thus, with the exception of the IS modes, we have found that these low-frequency modes can be generated by forcing the linearized BVE with fairly simple divergent wind fields that could easily be interpreted as the result of anomalous tropical convection. In the case of the HLM and SPW modes it is not quite so clear what gives rise to the anomalous convection, but in the case of the ENSO and MJO modes the source can be linked to divergence anomalies. Although several previous studies have demonstrated statistical links between tropical OLR anomalies and higher-latitude streamfunction anomalies, we felt it was useful to establish a robust dynamical link as well.

The fact that these modes explain between 7% (MJO) and 18% (ENSO) of the variance on these timescales suggests it may be possible to use them to make extended-range forecasts. If we could correlate the divergence patterns we have calculated (associated with the propagating MJO or SPW patterns) with the current or recent OLR fields, it may be possible to establish the current phase and amplitude of the respective modes. It may be possible to do this directly from the time coefficients of the streamfunction EOFs. With this knowledge we may then be able to predict the expected modulation of the 300-hPa streamfunction over the next season, by the passage of an ensemble of these modes. This will be the subject of further work.

The major significance of the work is to provide further evidence of the connection between tropical convection and higher-latitude streamfunction anomalies.

Acknowledgments. The barotropic vorticity equation model code was kindly supplied by the atmospheric modeling group at Reading University. We thank Lois Steenman-Clark who helped adapt it to run locally. The Data Services Section at NCAR provided the NCEP–NCAR reanalysis dataset. Thanks to Jim Renwick for helpful comments on an earlier draft. This research was funded by the New Zealand Foundation for Research, Science and Technology under Contract CO1628.

REFERENCES

Ambrizzi, T., and B. J. Hoskins, 1997: Stationary Rossby-wave propagation in a baroclinic atmosphere. *Quart. J. Roy. Meteor. Soc.,* **123,** 919–928.

Gill, A. E., 1980: Some simple solutions for heat induced tropical circulation. *Quart. J. Roy. Meteor. Soc.,* **106,** 447–462.
Hendon, H. H., 1986: The time mean flow and variability in a nonlinear model of the atmosphere with tropical diabatic forcing. *J. Atmos. Sci.,* **43,** 72–88.
Horel, J. D., and J. M. Wallace, 1981: Planetary-scale atmospheric phenomena associated with the Southern Oscillation. *Mon. Wea. Rev.,* **109,** 813–829.
Hoskins, B. J., and D. J. Karoly, 1981: Steady linear response of a spherical atmosphere to thermal and orographic forcing. *J. Atmos. Sci.,* **38,** 1179–1196.
——, and T. Ambrizzi, 1993: Rossby wave propagation on a realistic longitudinally varying flow. *J. Atmos. Sci.,* **50,** 1661–1671.
Jin, F., and B. J. Hoskins, 1995: The direct response to tropical heating in a baroclinic atmosphere. *J. Atmos. Sci.,* **52,** 307–319.
Kalnay, E., and Coauthors, 1996: The NCEP/NCAR 40-Year Reanalysis Project. *Bull. Amer. Meteor. Soc.,* **77,** 437–471.
Karoly, D. J., 1990: The role of transient eddies in low frequency zonal variations in the Southern Hemisphere circulation. *Tellus,* **42A,** 41–50.
Kidson, J. W., 1988: Interannual variations in the Southern Hemisphere circulation. *J. Climate,* **1,** 1177–1198.
——, 1999: Principal modes of Southern Hemisphere low frequency variability obtained from NCEP/NCAR reanalyses. *J. Climate,* **12,** 2808–2830.
——, and M. R. Sinclair, 1995: The influence of persistent anomalies on Southern Hemisphere storm tracks. *J. Climate,* **8,** 1938–1950.
Kiladis, G. N., and K. C. Mo, 1998: Interannual and intraseasonal variability in the Southern Hemisphere. *Meteorology of the Southern Hemisphere, Meteor. Monogr.*, No. 49, Amer. Meteor. Soc., 307–336.
Kousky, V. E., and G. D. Bell, 1992: *Atlas of Southern Hemisphere 500-mb teleconnection patterns derived from National Meteorological Center analyses.* NOAA Atlas No. 9, 90 pp.
Lau, K.-M., P.-J. Sheu, and I.-S. Kang, 1994: Multiscale low-frequency circulation modes in the global atmosphere. *J. Atmos. Sci.,* **51,** 1169–1193.
Madden, R. A., and P. Julian, 1972: Description of global scale circulation cells in the tropics with a 40–50 day period. *J. Atmos. Sci.,* **29,** 1109–1123.
Mitchell, T. P., and J. M. Wallace, 1996: ENSO seasonality: 1950–78 versus 1979–92. *J. Climate,* **9,** 3149–3161.
Mo, K. C., 1986: Quasi-stationary waves in the Southern Hemisphere. *Mon. Wea. Rev.,* **114,** 808–823.
——, and R. W. White, 1985: Teleconnections in the Southern Hemisphere. *Mon. Wea. Rev.,* **113,** 22–37.
——, and M. Ghil, 1987: Statistics and dynamics of persistent anomalies. *J. Atmos. Sci.,* **44,** 877–901.
——, and R. W. Higgins, 1998: The Pacific–South American modes and tropical convection during the Southern Hemisphere winter. *Mon. Wea. Rev.,* **126,** 1581–1596.
Rasmusson, E. M., and K. C. Mo, 1993: Linkages between 200-mb tropical and extratropical circulation anomalies during the 1986–1989 ENSO cycle. *J. Climate,* **6,** 595–616.
Renwick, J. A., and M. J. Revell, 1999: Blocking over the South Pacific and Rossby wave propagation. *Mon. Wea. Rev.,* **127,** 2233–2247.
Sardeshmukh, P. D., and B. J. Hoskins, 1987: On the derivation of the divergent flow from the rotational flow: The χ problem. *Quart. J. Roy. Meteor. Soc.,* **113,** 339–360.
——, and ——, 1988: The generation of global rotational flow by steady idealized tropical divergence. *J. Atmos. Sci.,* **45,** 1228–1251.
Trenberth, K. E., 1991: General characteristics of El Nino–Southern Oscillation. *Teleconnections Linking Worldwide Climate Anomalies*, M. H. Glantz, R. W. Katz, and N. Nicholls, Eds., Cambridge University Press, 13–42.
——, G. W. Branstator, D. Karoly, A. Kumar, N.-C. Lau, and C. Ropelewski, 1998: Progress during TOGA in understanding and modeling global teleconnections associated with tropical sea surface temperatures. *J. Geophys. Res.,* **103** (C7), 14 291–14 324.
Tyrrell, G. C., D. J. Karoly, and J. L. McBride, 1996: Links between tropical convection and variations of the extratropical circulation during TOGA COARE. *J. Atmos. Sci.,* **53,** 2735–2748.
Weickmann, K. M., G. N. Kiladis, and P. D. Sardeshmukh, 1997: The dynamics of intraseasonal atmospheric angular momentum oscillations. *J. Atmos. Sci.,* **54,** 1445–1461.